*Eng. & Tech. Journal, Vol. 30, No.3 , 2012*

# Shock Wave Capturing Numerically in Two-Dimensional Supersonic Wind Tunnel for Different Configurations

**Ahmed Fouad Mahdi**
Al-Kwarizmi Engineering College, University of Baghdad/Baghdad
Email:**afmkridi@hotmail.com**

**Received on: 3 /5 / 2011 & Accepted on: 1 /12/ 2011**

**ABSTRACT**

Numerical solutions of two dimensional Euler equations are obtained for transonic and supersonic flows. The shock capturing method is employed to solve compressible Euler equations by using MacCormack's time marching method that an explicit finite-difference technique. The test case chosen is that of a transonic and supersonic flow through a channel with a circular arc bump on the lower wall, half wedge and extended compression corner. Computational results accurately reproduced the flow field. In three cases, contour plots showing the important features of the flow-field are presented. The algorithm is tested for steady-state inviscid flows at different Mach numbers ranging from the transonic to the supersonic regime and the results are compared with the existing numerical solutions. The method incorporates bounded high resolution of discontinuities and is therefore well suited to all flow regimes ranging from transonic to supersonic.

**Keywords:** CFD, Euler Equation, Supersonic wind tunnel, MacCormack's technique.

## احتجاز الموجة الصدمية في نفق هوائي فوق صوتي ثنائي البعد ولأشكال مختلفة

**الخلاصة**

استخلاص الحل العددي للجريان الفوق الصوتي والانتقالي الثنائي البعد باستخدام معادلة أويلر للجريان. والاستفادة من طريقة احتجاز الموجة الصدمية لحل معادلة أويلر للجريان ألانضغاطي بطريقة تقنية ماكورماك وتوظيف طريقة الزحف الزمني لحل المعادلات التفاضلية المتحكمة في الجريان. تم الحصول على الحل العددي عن طريق تحويل المعادلات الحاكمة باستخدام طريقة الفروق المحددة. باختيار ثلاثة حالات لتغيير شكل الجدار السفلي من المجرى الهوائي باستخدام عثرة قوس الدائرة, وعثرة نصف الحافة الحادة وزاوية انضغاطيه ممتدة في الجدار السفلي للمجرى الهوائي. وكانت النتائج الحسابية دقيقة لحالات الجريان الثلاث, وتم رسم خطوط الانسياب والتي أوضحت ظواهر وميزات حقل الجريان. خوارزمية الاختبار طبقت على حالة الجريان المستقر غير اللزج ولقيم مختلفة من حدود أرقام ماخ وخاصة في الجريان فوق الصوتي وقورنت النتائج بالدراسات العددية المتوفرة. الطريقة المقدمة توفر دمج الحدود بدقة عالية لذلك فهي ملائمة لكل مناطق الجريان الانتقالي والفرق صوتي.

## INTRODUCTION

Shock boundary layer interaction is an important phenomenon in the aerodynamic design of high speed aircraft wings, and of turbine and cascade blades in turbomachinery and air breathing engine inlets and diffusers. Due to this, even in the numerical simulations, the general viscous flow in which flow separation occurs is of primary interest, in this paper, an attempt is made to study the shock capturing method to define the normal and oblige shock interaction on the test section. The algebraic grid generation technique used to build the computational domain, the simple mathematical concepts underlying in finite-difference methods make them easy to implement.

In flow fields involving shock waves, there are sharp, discontinuous changes in the primitive flow-field variables $p$, $\rho$, $u$, $T$, etc., across the shocks. Many computations of flows with shocks arc designed to have the shock waves appear naturally within the computational space as a direct, result of the overall flow-field solution, i.e., as a direct result of the general algorithm, without any special treatment to take care of the shocks themselves. Such approaches are called *shock-capturing method*.

The capturing of sharp gradients in compressible aerodynamic flows as well as shock waves and contact discontinuities has been the subject of many research and development. The work has resulted in the devising of various high-resolution schemes, notably the total variation diminishing (TVD) technique [1] and Jameson's artificial dissipation method [2]. Most of these schemes have been implemented in density-based numerical algorithms. Computational methods used in aerospace applications for the computation of compressible flows have reached a very high level of maturity with respect to accuracy and efficiency. Nowadays, there are two main approaches advocated in the development of algorithms for the computation of flow at all speeds; first, there is the modification of compressible solvers (density-based) downward to low Mach numbers; second, extending of the classical incompressible solvers (pressure-based) towards the compressible flow. Density-based algorithms without modification become impractical for low Mach number flows. Turkel et al. [3,4] and Guillard and Viozat [5] introduced the preconditioning techniques and identified that in the low Mach numbers, the discredited solution of the compressible fluid flow equations may fail to provide an accurate approximation to the incompressible flow equations. Also, in a recent work, Razavi and Zamzamian [6] presented an artificial compressibility method to solve the incompressible flow equations using a density-based algorithm as the work in this paper.

The shock capturing method is an ideal one for complex flow problems involving, shock waves for which we do not know either the location or number of shocks. Here, the shocks simply form within the computational domain as nature would have it. Moreover, this takes place without requiring

Any special treatment of the shock within the algorithm and hence simplifies the computer programming.

The problem of internal supersonic flow has the potential of being investigated endlessly. To calculate the flow properties in such flows, the solution technique should be able to handle the strong interactions resulting from any compressible flow phenomena like shockwave/expansion fan patterns in the solution domain. Recently many CFD research efforts ([7]-[8][15]S) were directed towards the development of such numerical techniques. These techniques should be able to operate on flow domains with shockwaves without altering the solution accuracy.

## GOVERNING EQUATIONS

For high Reynolds number flow, viscous effects are confined to the vicinity of the surface, where large velocity gradients exist. This region is known as the boundary layer. Outside the boundary layer, the velocity gradients are negligible resulting in zero shear stresses. This region is called the inviscid region, and solution procedures for the inviscid flow region are governed by the Euler equations and the solution of this research depends on it, which is written in conservation-law form for two-dimensional flows of a perfect gas [22]. The general compact vector form is given as:-

$$\frac{\partial U}{\partial t} + \frac{\partial E}{\partial x} + \frac{\partial F}{\partial y} = 0$$

$$U = \begin{bmatrix} r \\ ru \\ rv \\ re_t \end{bmatrix}, \quad E = \begin{bmatrix} ru \\ ru^2 + p \\ ruv \\ u(e_t + p) \end{bmatrix}, \quad F = \begin{bmatrix} rn \\ run \\ rn^2 + p \\ n(e_t + p) \end{bmatrix} \text{-(2-1)}$$

Where: $u$ and $v$ are the velocities along the $x$ and $y$ coordinates, respectively, $p$ is the pressure, $r$ is the density, and et is the total energy per unit volume. And $U$, $E$, $F$, are the fluxes vectors.

The governing equation in a conservation form could be written as continuity Equation given in [17]. $r$, $u$, $v$, $p$ and $e$ are a (primitive variables) non dimensional density, velocity in $x$-direction, velocity in $y$-direction, pressure and internal energy respectively.

The time step ($Dt$) cannot be arbitrary, rather it must be less than some maximum values for stability, it was stated that $Dt$ must obey the Courant-Friedriches-Lowry criterion $CFL$. The $CFL$ criterion states that physically the explicit time step must be not greater than the time required for a sound wave to propagate from one grid to next. The maximum allowable value of $CFL$ factor for stability in explicitly time dependent finite difference calculation can vary from approximately 0.5 to 0.1. To determine the value of time step, the following version of the $CFL$ criterion [17] is used. Where $a_{i,j}$ is the local speed of sound in meters per second, and $C$ is the constant number.

$$(\Delta t_{CFL})_{i,j}=\left[\left|\frac{u_{i,j}}{\Delta\xi}\right|+\left|\frac{v_{i,j}}{\Delta\eta}\right|+a_{i,j}\sqrt{\frac{1}{\Delta\xi^2}+\frac{1}{\Delta\eta^2}}\right]^{-1} \quad \ldots\ldots(2\text{-}2)$$

and: *Dt = min* [*C (Dt CFL) i,j*] .

## COMPUTATIONS TECHNIQUE

The MacCormack's time marching method is an explicit finite-difference technique. It is second-order-accurate in both space and time. The results obtained by using MacCormack's method are perfectly satisfactory for many fluid flow applications [17]. A developed technique employs time-marching solution technique for numerically solving the time dependent Euler Equation. The main factors that influence this choice are the ability to use the same difference operator in both subsonic and supersonic regions of the flow field. To solve the finite difference pertaining, the MacCormack's predictor-corrector technique was used. The main geometric parameters of the supersonic inlet are referred to Figure (3.1).

## BOUNDARY CONDITIONS

At the inlet of the domain, all flow variables are specified if the flow is supersonic. For subsonic inlet flow, only three of the four variables need to be prescribed: the total temperature, the angle of attack, and the total pressure. At the outlet, all of the flow variables are obtained by linear extrapolation for supersonic velocities; the pressure is fixed when the outlet is subsonic. Slip boundary conditions are used on the lower and upper walls of the bump in the inviscid flow test cases.

The Euler equation has an unlimited number of solutions. What makes a solution unique is the proper specification of initial and boundary conditions for a given PDE (Euler equation). A set of boundary conditions must be specified, it referred to as the "analytical boundary condition" Once the PDE is approximated by a FDE, Thus the FDE will require additional boundary conditions. This boundary condition will be referred to as "numerical boundary condition".

### Solid Boundary Condition

For the three solid boundary conditions (ramp, inside and outside cowl), the tangency grid body surface must be satisfied for inviscid flow. The components of the momentum equation for the two-dimension flow may be expressed with some mathematical steps, as [18]:-

$$\left.\begin{aligned}&\eta_x\left(\frac{\rho u\overline{U}}{J}\right)_\xi+\eta_y\left(\frac{\rho u\overline{U}}{J}\right)_\xi+\eta_x\left(\frac{\rho v\overline{V}}{J}\right)_\eta+\eta_x\left(\frac{\rho u\overline{V}}{J}\right)_\eta\\&+\eta_x\left(\frac{\xi_x P}{J}\right)_\xi+\eta_x\left(\frac{\eta_x P}{J}\right)_\eta+\eta_y\left(\frac{\xi_y P}{J}\right)_\xi+\eta_y\left(\frac{\eta_y P}{J}\right)_\eta=0\end{aligned}\right\} \quad \ldots. (4\text{-}1)$$

Where $\overline{U}$ is the tangential velocity in the computational domain, and $\overline{V}$ is the normal velocity at the surface in the computational domain is equal to zero. There are two kinds of the solid boundaries they are:-

### The lower Solid Surface

For the lower surface, a finite difference equation for (4-1) equation is obtained, as a second order central difference approximation for the *x* derivatives and a second order forward difference approximation for *h* derivatives are used as illustrated in Fig. 4.1.1.

Note that the unknowns are the values of pressure at soled surfaces. The value at the interior points has already been computed with the second order approximation by predictor step and corrector step of MacCormack's method. The finite difference equation is obtained as:

$$\frac{h_{x_{i,j}}}{2\Delta x}\left[\left(\frac{r u \bar{U}}{J}\right)_{i+1,j}-\left(\frac{r u \bar{U}}{J}\right)_{i-1,j}\right]$$
$$+\frac{h_{y_{i,j}}}{2\Delta x}\left[\left(\frac{r u \bar{U}}{J}\right)_{i+1,j}-\left(\frac{r u \bar{U}}{J}\right)_{i-1,j}\right]$$
$$+\frac{h_{x_{i,j}}}{2\Delta h}\left[-3\left(\frac{r u \bar{V}}{J}\right)_{i,j}+4\left(\frac{r u \bar{V}}{J}\right)_{i,j+1}-\left(\frac{r u \bar{V}}{J}\right)_{i,j+2}\right]$$
$$+\frac{h_{x_{i,j}}}{2\Delta h}\left[-3\left(\frac{r v \bar{V}}{J}\right)_{i,j}+4\left(\frac{r u \bar{V}}{J}\right)_{i,j+1}-\left(\frac{r v \bar{V}}{J}\right)_{i,j+2}\right]$$
$$+\frac{h_{x_{i,j}}}{2\Delta x}\left[\left(\frac{x_x p}{J}\right)_{i+1,j}-\left(\frac{x_x p}{J}\right)_{i-1,j}\right]$$
$$+\frac{h_{x_{i,j}}}{2\Delta h}\left[-3\left(\frac{h_x p}{J}\right)_{i,j}+4\left(\frac{h_x p}{J}\right)_{i,j+1}-\left(\frac{h_x p}{J}\right)_{i,j+2}\right]$$
$$+\frac{h_{y_{i,j}}}{2\Delta x}\left[\left(\frac{x_y p}{J}\right)_{i+1,j}-\left(\frac{x_y p}{J}\right)_{i-1,j}\right]$$
$$+\frac{h_{y_{i,j}}}{2\Delta h}\left[-3\left(\frac{h_y p}{J}\right)_{i,j}+4\left(\frac{h_y p}{J}\right)_{i,j+1}-\left(\frac{h_y p}{J}\right)_{i,j+2}\right] \quad \ldots\ldots(4\text{-}2)$$
$$=0$$

The value of normal velocity $\bar{V}$ is zero at the lower solid surface, therefore; this equation is regrouped so that a tridiagonal system is formed. The rearrangement is as follows:-

$$a_i p_{i-1,j}+b_i p_{i,j}+c_i p_{i+1,j}=d_i \quad \text{--(4-3)}$$

Where:

$$a_i=-\frac{1}{2\Delta x}\left[h_{x_{i,j}}\left(\frac{x_x}{J}\right)_{i-1,j}+h_{y_{i,j}}\left(\frac{h_y}{J}\right)_{i-1,j}\right]$$

$$b_i=-\frac{3}{2\Delta h}\left[\frac{h_x^2+h_y^2}{J}\right]_{i,j}$$

$$d_i = \frac{P_{i,j+2}}{2\Delta h}\left[h_{x\,i,j}\left(\frac{h_x}{J}\right)_{i,j+2} + h_{y\,i,j}\left(\frac{h_y}{J}\right)_{i,j+2}\right]$$

$$c_i = \frac{1}{2\Delta x}\left[h_{x_{i,j}\,i,j}\left(\frac{x_x}{J}\right)_{i+1,j} + h_{y_{i,j}}\left(\frac{x_y}{J}\right)_{i+1,j}\right] - \frac{2P_{i,j+2}}{\Delta h}\left[h_{x\,i,j}\left(\frac{h_x}{J}\right)_{i,j+1} + h_{y\,i,j}\left(\frac{h_y}{J}\right)_{i,j+1}\right]$$
$$- \frac{2}{\Delta h}\left(\frac{r\bar{V}}{J}\right)_{i,j+1}\left[h_{x\,i,j}u_{i,j+1} + h_{y\,i,j}v_{i,j+1}\right]$$
$$+ \frac{1}{2\Delta h}\left(\frac{r\bar{V}}{J}\right)_{i,j+2}\left[h_{x\,i,j}u_{i,j+2} + h_{y\,i,j}v_{i,j+2}\right]$$
$$+ \frac{1}{2\Delta x}\left(\frac{r\bar{U}}{J}\right)_{i-1,j}\left[h_{x\,i,j}u_{i-1,j} + h_{y\,i-1,j}v_{i-1,j}\right]$$
$$- \frac{1}{2\Delta x}\left(\frac{r\bar{U}}{J}\right)_{i+1,j}\left[h_{x\,i,j}u_{i+1,j} + h_{x\,i,j}v_{i+1,j}\right]$$

**The Upper Solid Surface**

For the upper surface $\bar{V}$ =0, and from Equation (4-1), a second order central difference approximation for ξ derivatives and second-order backward difference approximation for η derivatives are used as illustrated in Fig. (4.1.2).

Finding the pressure at the lower surface of cowl, for nonporous surface (normal velocity V=0.), the tridiagonal system is found. The arrangement for the lower cowl surface is as follows:-

$$a_i p_{i-1.j} + b_i p_{i.j} + c_i p_{i+1.j} = d_i \quad \text{---- (4-4)}$$

Where: $a_i = -\frac{1}{2\Delta x}\left[h_{x\,i,j}\left(\frac{x_x}{J}\right)_{i-1,j} + h_{y\,i,j}\left(\frac{h_y}{J}\right)_{i-1,j}\right]$

$$b_i = -\frac{3}{2\Delta h}\left[\frac{h_x^2 + h_y^2}{J}\right]_{i,j} \qquad c_i = -\frac{1}{2\Delta x}\left[h_{x_{i,j}}\left(\frac{x_x}{J}\right)_{i+1,n_1} + h_{y_{i,j}}\left(\frac{x_y}{J}\right)_{i-1,j}\right]$$

$$d_i = -\frac{P_{i,j+2}}{2\Delta h}\left[h_{x\,i,j}\left(\frac{h_x}{J}\right)_{i,j+2} + h_{y\,i,j}\left(\frac{h_y}{J}\right)_{i,j+2}\right]$$
$$+ \frac{2P_{i,j+2}}{\Delta h}\left[h_{x\,i,j}\left(\frac{h_x}{J}\right)_{i,j+1} + h_{y\,i,j}\left(\frac{h_y}{J}\right)_{i,j+1}\right]$$
$$+ \frac{2}{\Delta h}\left(\frac{r\bar{V}}{J}\right)_{i,j+1}\left[h_{x\,i,j}u_{i,j+1} + h_{y\,i,j}v_{i,j+1}\right]$$
$$- \frac{1}{2\Delta h}\left(\frac{r\bar{V}}{J}\right)_{i,j+2}\left[h_{x\,i,j}u_{i,j+2} + h_{y\,i,j}v_{i,j+2}\right]$$
$$+ \frac{1}{2\Delta x}\left(\frac{r\bar{U}}{J}\right)_{i-1,j}\left[h_{x\,i,j}u_{i-1,j} + h_{y\,i-1,j}v_{i-1,j}\right]$$
$$- \frac{1}{2\Delta x}\left(\frac{r\bar{U}}{J}\right)_{i+1,j}\left[h_{x\,i,j}u_{i+1,j} + h_{x\,i,j}v_{i+1,j}\right]$$

To solve Equations (4-3) and (4-4), the tridiagonal matrix solver system is obtained at j=1 on the lower surface and j=70 at the upper surface shown in [18].

The velocity component in computational domain at the soled surface is, $C_i$, $D_i$, for a perfect gas and the calculation equation to find the density at the wall could write as:

$$r_{i,1} = \frac{2g\ p_{i,1} + \sqrt{4g^2 P_i^2 + 8(h_t)_{wall}\,(g-1)^2 (C^2{}_i + D^2{}_i)}}{4(g-1)(h_t)_{wall}}\ \gamma: \quad \text{.....(4-5)}$$

Air specific heat ratio, taken as ($\gamma$=1.4).

$$(h_t)_{wall} = t_{inf}.c_p + \frac{1}{2}u_{inf}^2 \quad \text{....(4-6)}$$

Note that the positive sign is used exclusively to prevent negative density value.

## 5. NUMERICAL RESULTS

The first validation is the flow over a bump in the channel geometry in which transonic and supersonic flows were computed by shock capturing methods and compared together and with the other existing numerical predictions, including pressure-based or density-based methods. Many problems have been solved to validate the applicability and effectiveness of the shock capturing method in the solution of supersonic internal flow problems. In all cases the method showed good agreement with analytical solutions, if any, and with the published literature. All the test cases have been solved using FORTRAN 90 code a preconditioned tridiagonal matrix solver. The reader is referred to [18] for more details. In this section we present three test cases.

### A. Circular Arc Problem

Flow over an arc bump is a typical problem used to validate various algorithms for all Mach number flows. The circular arc problem is shown in Figure 5.1.

The circular arc maximum height is set to 0.04. The solution domain is discretized using 120×80 uniform bilinear quadrilateral elements. The inlet boundary is supersonic and the following values have been used: Mach number =0.9, 1.0,1.25, 1.4, 1.5, 1.65 & P=101325Pa, T=288K

The no-penetration boundary condition is applied on both the upper and lower boundaries and the exit boundary is left free being supersonic. Figure 5.2 shows the

Fig.5.1. Circular Arc

Mach No. contours. The show results match very well the results given in [21] and [23].

Figures 5.2 present the solutions for subsonic, transonic and supersonic flows (M = 0.9, 1.0, 1.25, 1.4, 1.5, 1.65) for circular arc bumps in a channel, used in the computations. Although the mathematical model is simpler than the Navier–Stokes equations, the presence of discontinuities and their interactions (shock–shock interaction and shock reflection) serves as a good test for the capabilities of the method to resolve shockwaves and their interactions.

The constant Mach number contours are chosen to compare the resolution of shock waves for these schemes. The results of Jameson's scheme in the density-based algorithm on a grid of 145×33 nodes [24], a total variation diminishing (TVD) scheme in a pressure-based algorithm on a grid of 90 × 30 [25] for the case M = 1.4, and the results for ref. [26] are shown in Fig. 5.2.1.b, d and c respectively. As it can be seen from these figures, all shock structures are very well resolved by the shock capturing method.

**B. Extended Compression Corner Problem**

The extended compression corner problem is shown in Figure 5.3. The solution domain is discretized using 210×70 uniform bilinear quadrilateral elements.
The inlet boundary is supersonic and the following values have been used:

Mach number =0.9, 1.0, 1.25, 1.4, 1.5, 1.65 & P=101325Pa, T=288K

Again the no-penetration boundary condition is applied on both the upper and lower boundaries and the exit boundary is left free being supersonic. Figure 5.4 shows the Mach No. contours. The show results match very well the results of the analytical solution given from the oblique shock wave theory.

**C. Half Wedge in a Supersonic Wind Tunnel**

The solution domain of a half wedge, as shown in Figure 5.5, is discretized uniformly with 210×70 bilinear rectangular elements. At the inlet boundary, the transonic and supersonic inlet boundary condition is used with the following values:

Mach number =0.9, 1.0, 1.25, 1.4, 1.5, 1.65 & P=101325Pa, T=288K

On lower boundary and upper boundaries, the inviscid wall (no-penetration) boundary condition is used and the exit boundary is left free being supersonic exit. Figure 5.6 shows the Mach No.( 0.9, 1.0, 1.25, 1.4, 1.5, 1.65) contours. Our results match the results obtained from the oblique shockwave theory.

## CONCLUSIONS

The shock capturing method (density-based) is capable of recovering the implicitness parameters for the transonic and supersonic internal flow problems by used a computer program written in **FORTRAN 90** based on McCormack's technique was used to perform the objectives of this work, it gave a satisfactory performance in all the tested problems, and with the same algorithm, the presented method has an excellent resolution of flows under serve conditions (simple shocks, shock reflection, shock/shock interaction, etc.). The agreement between the results of the presented implementation of the method scheme and those of the other schemes such as pressure-based methods is excellent, as perhaps expected.

## REFERENCES

[1]. Harten, A.: High resolution scheme for hyperbolic conservation laws. J. Comput. Phys. 49(3), 357–393 (1983)
[2]. Jameson, A., Schmidt, W., Turkel, E.: Numerical solutions of the Euler equations by finite-volume methods using Runge–

Kutta time-stepping schemes. AIAA, Paper 81-1259, June (1981)
[3]. Turkel, E.: Preconditioned methods for solving the incompressible and low speed compressible equations. J. Comput.
Phys. 72, 277–298 (1987)
[4]. Turkel, E., Radespiel, R., Kroll, N.: Assessment of preconditioning methods for multidimensional aerodynamics. Comp.
Fluids 26(6), 613–634 (1997)
[5]. Guillard, H., Viozat, C.: On the behaviour of upwind schemes in the low Mach number limit. Comp. Fluids 28(1),
63–86 (1999)
[6]. Zamzamian, K., Razavi, S.E.: Multidimensional upwinding for incompressible flows based on characteristics. J. Comput.
Phys. 227(19), 8699–8713 (2008)
[7]. A.A. Megahed, M.W. El-Mallah, B.R. Girgis, A modified flowfield dependent variation method applied to the compressible Euler flow equations, Eights Int. Congress of Fluid Dynamics and Propulsion, ICFDP8-EG-102, 2006.
[8]. Chung, T.J., Transitions and interactions of inviscid/viscous, compressible/incompressible and laminar/turbulent flows, Int. J. Num. Meth. Fluids, vol. 31, pp. 223-46, 1999.
[9]. Schunk, R.G., Gunabal, Heard, G.W., and Chung, T.J., Unified CFD methods via flowfield-dependent variation theory, AIAA 99 (1999)-3715.
[10]. Yoon, K.T. and Chung, T.J., Three dimensional mixed explicit-implicit generalized Galerkin spectral elements methods for high speed turbulent compressible flows, Comp. Meth. Appl. Mech. Eng., vol. 135, pp. 343-67, 1996.
[11]. K.T. Yoon, S.Y. Moon, S.A. Garcia, G.W. Heard, T.J. Chung, Flowfield-dependent mixed explicit (FDMEI) methods for high and low speed and compressible and incompressible flows, Comp. Meth. Appl. Mech. Eng. 151 (1998), 75-104.
[12]. F. Shakib, Thomas J.R. Hughes. Zdenek Johan, A new finite element formulation for computational fluid dynamics: X. The compressible Euler and Navier-Stokes equations, Comp. Meth. Appl. Mech. Eng., vol. 89, pp. 141-219, 1991.
[13]. F. Moussaoui, A unified approach for inviscid compressible and nearly incompressible flow by least-squares finite element ethod, Appl. Num. Math., vol. 44, pp. 183-199, 2003.
[14]. G.J. Le Beau, T.E. Tezduyar, Finite element computations of compressible flows with the SUPG formulation, ASME, FED. vol. 123, Advances in finite element analysis in fluid dynamics, 1991.
[15] F. Taghaddosi, W.G. Habashi, G. Guevremont, and D. Ait-Ali-Yahia, An adaptive least square method for the compressible Euler equations, AIAA-97-2097, 1997.
[16]. K. M. Shimabukuro , Inlet Design Studies for a Mach 2.2 Advanced Supersonic Cruise Vehicle, Journal of aircraft; transaction of AIAA; Vol. 19; No. 7; July 1982.
[17]. JOHN. D. ANDERSON, TR., "Computational Fluid Dynamics", Department of Aerospace Engineering University of Maryland, McGraw-Hill, New York, International Editions 1995.

[18]. KLAUS A. HOFFMANN, "Computational Fluid Dynamics for Engineers". The University of Texas at Austin, A Publication of Engineering Education SystemTM, Austin, Texas 78713,USA.

[19]. B.R. Girgis, Flowfield-Dependent Variation Method Applied to Compressible Euler Flow Equations, Master Thesis, Eng. Mathematics and Physics Dept., Cairo University, Giza, Egypt, 2007.

[20]. A.A. Megahed, M.W. El-Mallah, B.R. Girgis, A modified flow field dependent variation method applied to the compressible Euler flow equations, Eights Int. Congress of Fluid Dynamics and Propulsion, ICFDP8-EG-102, 2006.

**[21].** F. Moussaoui, *A unified approach for inviscid compressible and nearly incompressible flow by least-squares finite element method*, Appl. Num. Math., vol. 44, pp. 183-199, 2003.

**[22].** G.J. Le Beau, T.E. Tezduyar, *Finite element computations of compressible flows with the SUPG formulation*, ASME, FED. vol. 123, Advances in finite element analysis in fluid dynamics, 1991.

[**23**] F. Taghaddosi, W.G. Habashi, G. Guevremont, and D. Ait-Ali-Yahia, *An adaptive least square method for the compressible Euler equations*, AIAA-97-2097, 1997.

[24]Arnone, A., Swanson, R.C.: A navier–stokes solver for cascade flows. NASA CR 181682, ICASE Report No. 88-32 (July1988).

[25]Issa, R.I., Javareshkian, M.H.: Pressure-based compressible calculation method utilizing total variation diminishing schemes. AIAA J. **36**(9), 1652–1657 (1998).

[26] M. H. Djavareshkian · M. H. Abdollahi Jahdi Shock-capturing method using characteristic-based dissipation filters in pressure-based algorithm 13 March 2009 © Springer-Verlag 2009.

## Nomenclature

| Symbol | Definition | Units |
|---|---|---|
| a | Speed of sound | $m^2$ |
| CFL | Courant Friedrichs Lewry number of Stability. | m/s |
| $D_i$ , $C_i$ | Velocity components in computational domain | |
| $c_x$, $c_y$ | Artificial viscosity coefficient in x and y. | |
| e | Specific internal energy. | J/kg |
| $e_t$ | Total energy | J/kg |
| $\overline{E}$, $\overline{F}$, $\overline{V}$ | Column vector in Cartesian coordinate | |
| E, F, V | Column vector in body filled coordinate | |
| $E_1$,…$E_4$ $F_1$,...$F_4$ $U_1$,…$U_4$ | Flux vector | |
| J | Jacobian of coordinate transformation. | |
| M | Mach number. | |
| $m^{\circ}$ | Mass flow rates. | kg/sec |
| P | Static pressure. | $N/m^2$ |
| $P_o$ | Stagnation pressure. | $N/m^2$ |
| t | Time | |
| u, v | Velocity component in x,y Coordinate direction | m/s |
| $\overline{U}$ | Conservation velocity component in *h* coordinate direction. | |
| $\overline{V}$ | Conservation velocity component in *x* coordinate direction. | |
| n | Unit normal vector. | |
| $\Delta t$ | Time step | |
| $\Delta x$, $\Delta y$ | Spatial steps in physical domain | |
| $\Delta\xi$, $\Delta\eta$ | Spatial steps in computational domain | |
| $\xi$, $\eta$ | Computational coordinates. | |
| i , j | Node indices indicate position in the x, y direction. | Subscript |
| x , y | Spatial derivative | Subscript |
| av. | Average | Subscript |
| o | Total condition | Subscript |
| $\xi$, $\eta$ | Computational derivative | Subscript |
| $\infty$ | Undisturbed air station | Subscript |
| t | Time level | superscript |
| $t+\Delta t$ | Next time level | superscript |

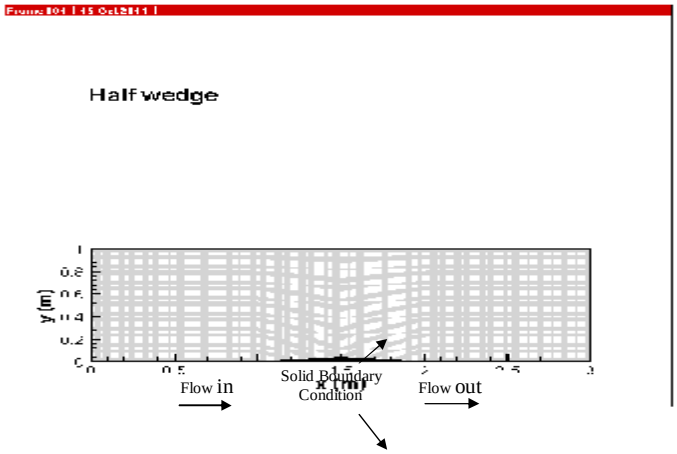


**Figure (3.1) the computational domain geometry with the types of boundaries**

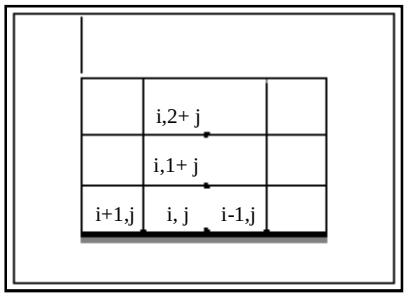


**Figure (4.1.1) Lower solid**

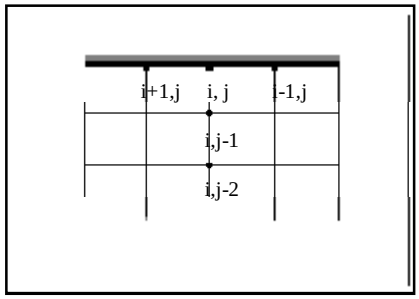


**Figure (4.1.2) Upper solid surface**

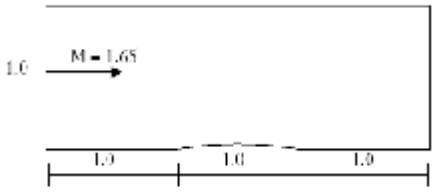


Figure (5.1.) Circular Arc

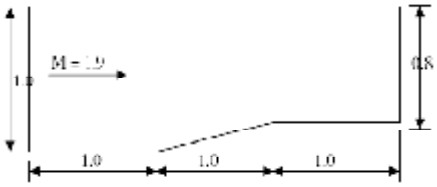


**Figure(5.3.) Extended Compression Corner**

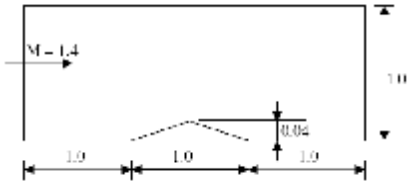


**Figure (5.5.) Half wedge**

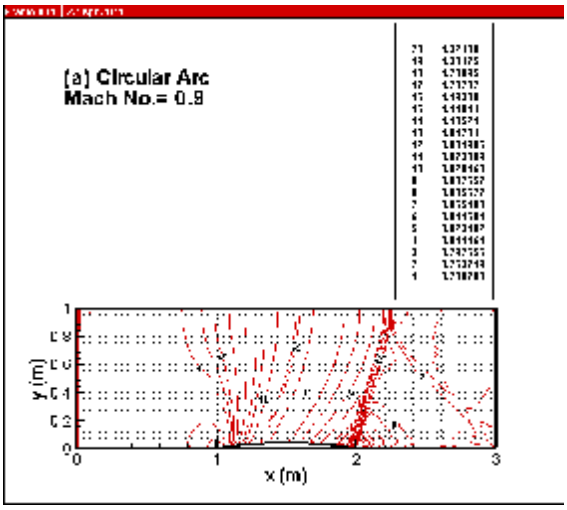


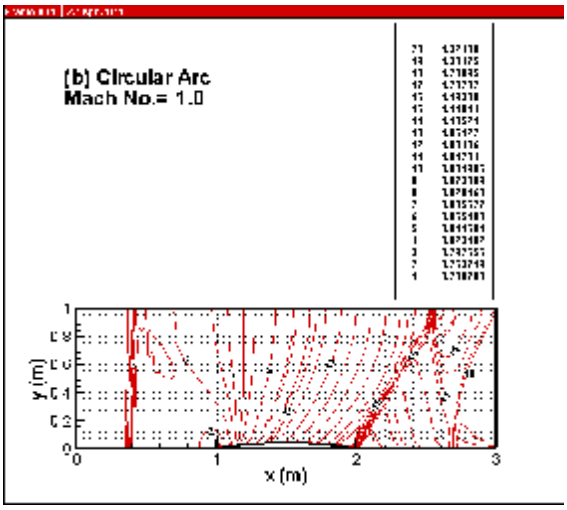


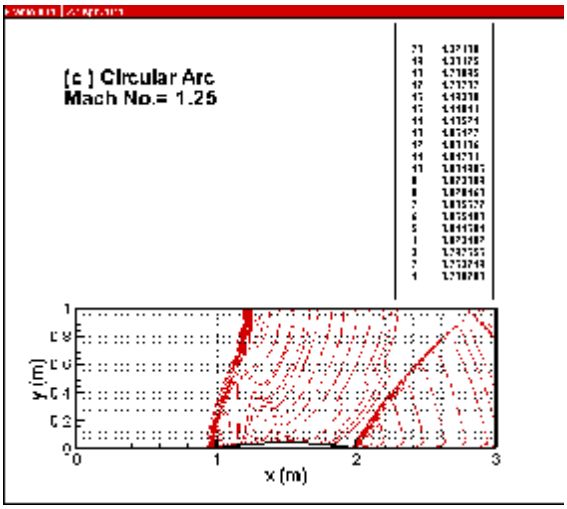


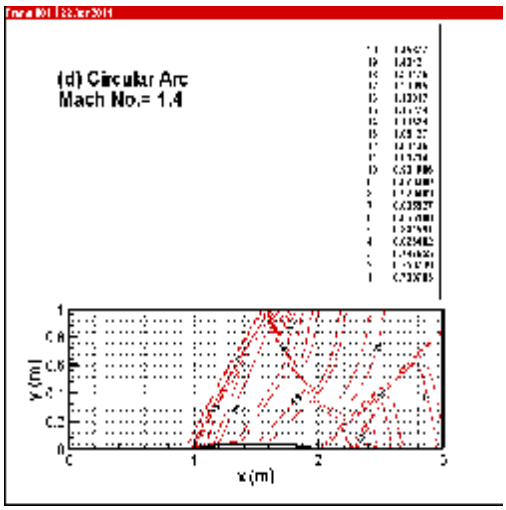


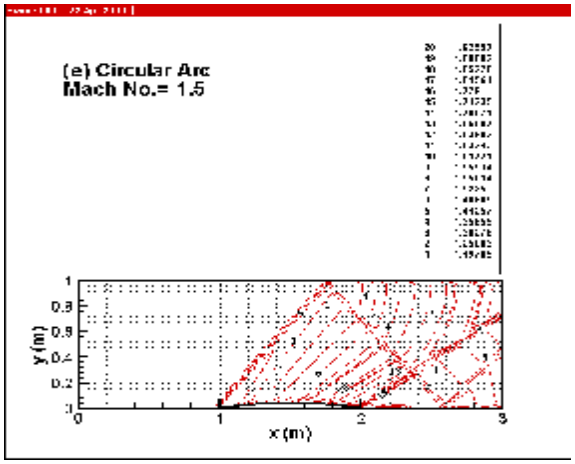


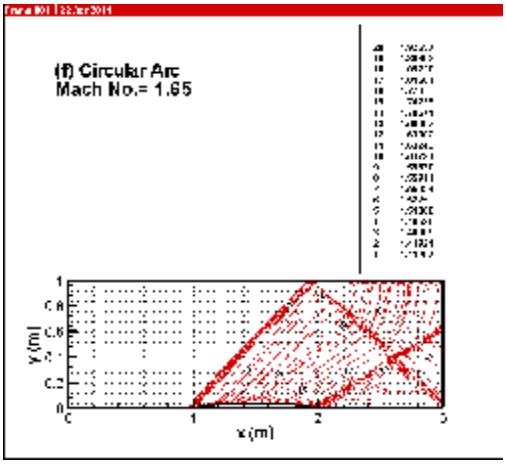

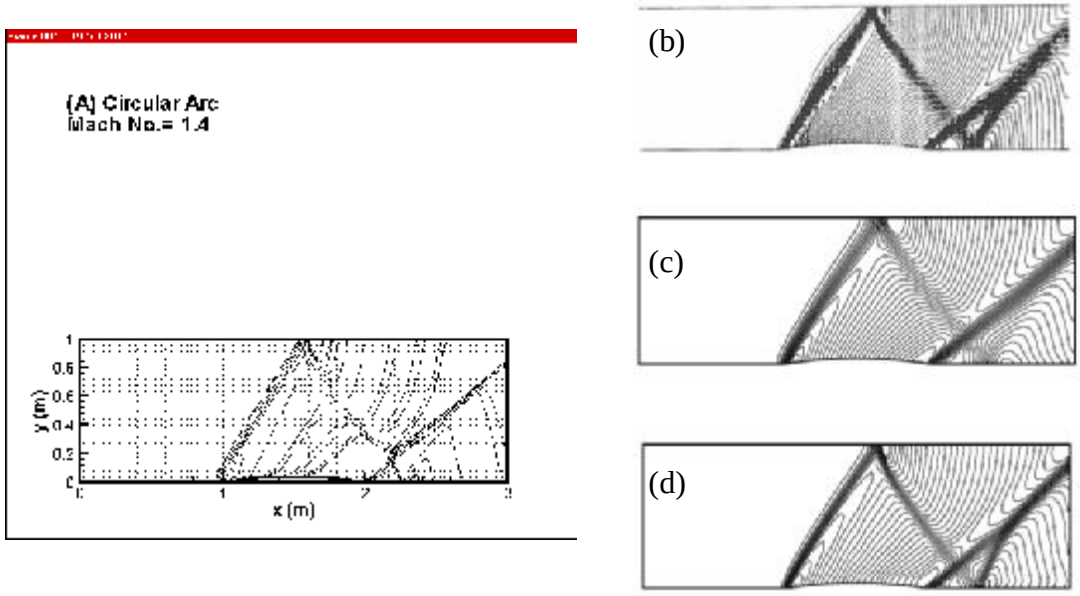


**Figure (5.2.1) (a) Supersonic flow over circular arc, inlet M=1.4 (present work) 120×80 mesh. (b) Mach contours [24]. (c) Mach contours (TVD) [25]. (d) Mach contours [26].**

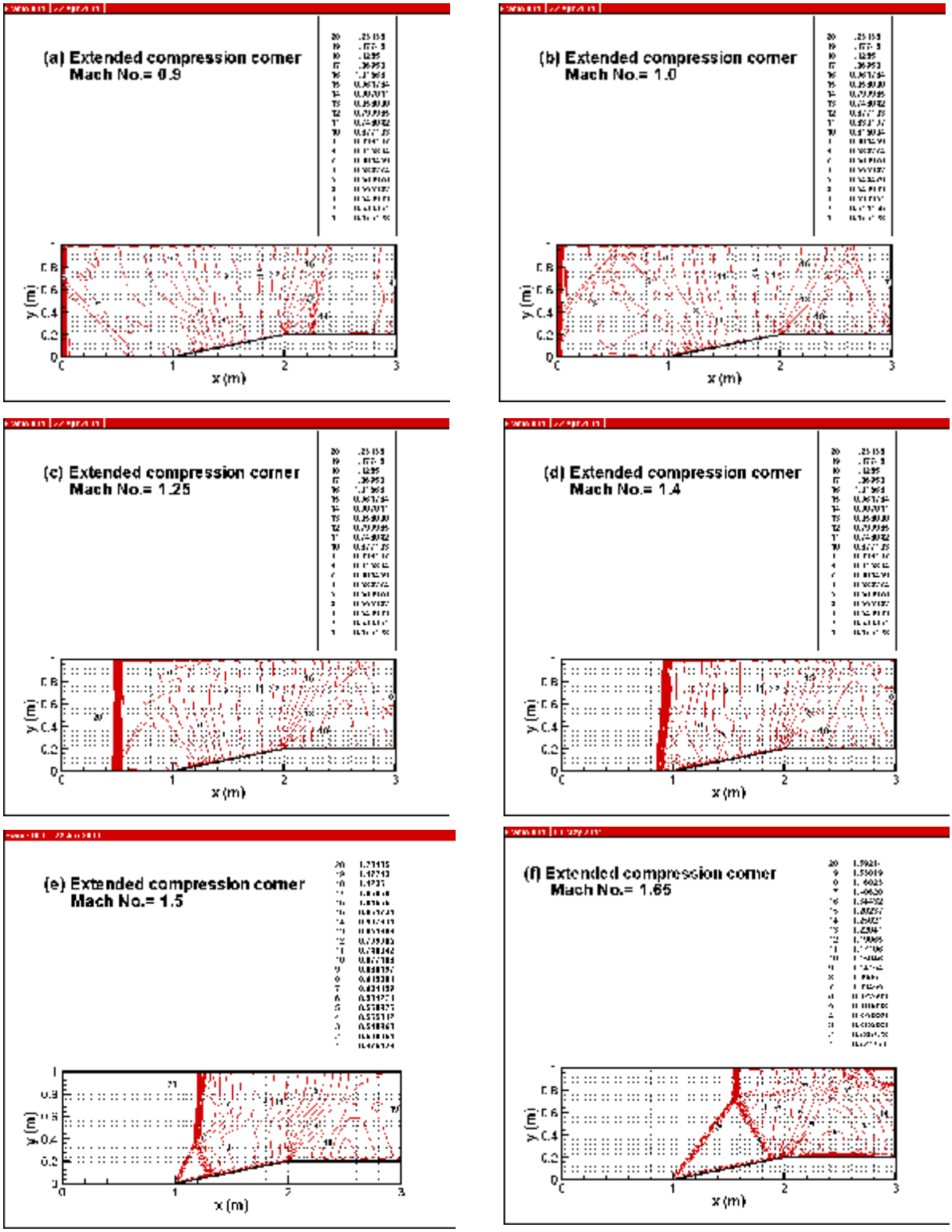


**Figure(5.4) Extended Compression corner**

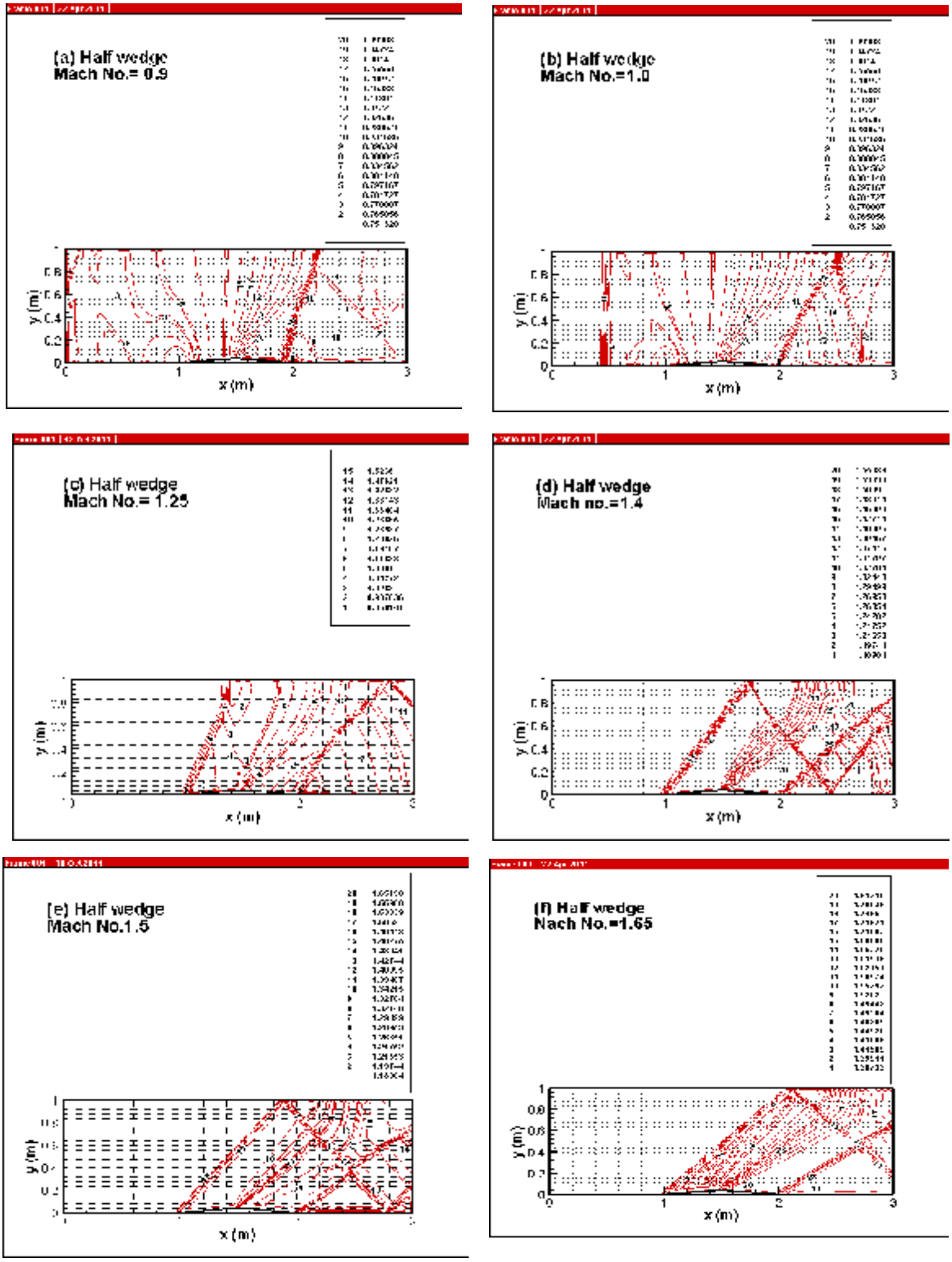


**Figure (5.6) Half xxedge**